

Optimal perturbations and streak spacing in wall-bounded turbulent shear flow

Kathryn M. Butler and Brian F. Farrell

Division of Applied Sciences, Harvard University, Cambridge, Massachusetts 02138

(Received 6 April 1992; accepted 30 June 1992)

The mean streak spacing of approximately 100 wall units that is observed in wall-bounded turbulent shear flow is shown to be consistent with near-wall streamwise vortices optimally configured to gain the most energy over an appropriate turbulent eddy turnover time. The streak spacing arising from the optimal perturbation increases with distance from the wall and is nearly independent of Reynolds number, in agreement with experiment.

A well-established characteristic of wall-bounded turbulent shear flow is the presence near the wall of regions of high- and low-speed fluid that are elongated in the streamwise direction and alternate in the spanwise direction. These streaky structures are observed to play an important role in the maintenance of turbulence through the ‘‘bursting’’ process, which is responsible for most of the turbulent kinetic energy production in the boundary layer.^{1,2}

The observed mean spanwise spacing between low-speed streaks is consistently found to be $\lambda_z^+ \approx 100$ wall units. The superscript + indicates quantities scaled by wall variables, according to which distance and time are nondimensionalized as $y^+ = yu_\tau/\nu$ and $t^+ = tu_\tau^2/\nu$, where ν is the kinematic viscosity and $u_\tau = [\nu(dU/dy)|_w]^{1/2}$ is the friction velocity, the subscript w denoting a value at the wall. The distribution of streak spacings is broad, with the coefficient of variation $\psi_\lambda = \sigma_\lambda^+ / \lambda_z^+ \approx 0.30\text{--}0.40$, where σ_λ^+ is the standard deviation.³ The mean streak spacing is observed to increase with distance from the wall,^{3,4} and is essentially independent of Reynolds number.³

It is generally accepted that the streak formation mechanism is linear and arises from the redistribution of mean momentum by streamwise rolls. This is evident, for example, in the comparison by Lee *et al.*⁵ of turbulent fields resulting from direct numerical simulation (DNS) to those developed using the linearized equations of rapid distortion theory (RDT) from the same initially isotropic turbulent field. It is reasonable, therefore, to ask whether the scale selection responsible for the observed streak spacing also arises from linear theory. An attempt by Waleffe and Kim⁶ to obtain the characteristic scale using the linear theories of selective amplification⁷ and direct resonance⁸ was unsuccessful, leading them to propose that the selection mechanism must be nonlinear and self-sustaining. In this work, we use optimal perturbation theory to show that the 100⁺ streak spacing is consistent with linear growth limited by turbulent disruption.

Optimal perturbation theory seeks the linear perturbations in a given background flow that grow by the largest amount in a chosen norm over a specified period of time. Mathematical details are presented in full in a recent paper.⁹ In brief, an arbitrary three-dimensional disturbance that is periodic in the spanwise z and streamwise x directions can be represented as a sum of eigenmodes

$$\begin{aligned} v &= \sum_j \gamma_j [\tilde{v}_j \exp(\sigma_j t)] \exp[i(\alpha x + \beta z)] \\ &= \mathbf{V} \boldsymbol{\gamma} \exp[i(\alpha x + \beta z)], \\ \omega &= \sum_j \gamma_j [\tilde{\omega}_j \exp(\sigma_j t)] \exp[i(\alpha x + \beta z)] \\ &= \boldsymbol{\Omega} \boldsymbol{\gamma} \exp[i(\alpha x + \beta z)], \end{aligned} \tag{1}$$

where the vertical velocity eigenmodes \tilde{v} solve the Orr–Sommerfeld equation and the vertical vorticity eigenmodes $\tilde{\omega}$ solve the associated Squire equation driven by \tilde{v} . The coefficient γ_j represents the spectral projection on mode j . Because the linearized Navier–Stokes operator is non-self-adjoint in the energy norm, certain perturbations may experience growth even in the absence of unstable eigenmodes. Writing the energy density \mathcal{E} as a quadratic form on the spectral projection $\boldsymbol{\gamma}$,

$$\begin{aligned} \mathcal{E} &\propto \left[\boldsymbol{\gamma}^* \mathbf{V}_t^* \mathbf{V}_t \boldsymbol{\gamma} + \frac{1}{(\alpha^2 + \beta^2)} \left(\boldsymbol{\gamma}^* \frac{\partial \mathbf{V}_t^*}{\partial y} \frac{\partial \mathbf{V}_t}{\partial y} \boldsymbol{\gamma} + \boldsymbol{\gamma}^* \boldsymbol{\Omega}_t^* \boldsymbol{\Omega}_t \boldsymbol{\gamma} \right) \right] \\ &= \boldsymbol{\gamma}^* \mathbf{E}_t \boldsymbol{\gamma}, \end{aligned} \tag{2}$$

the variational problem for the perturbation with maximum energy at time τ given unit initial energy results in the Euler–Lagrange equation

$$\mathbf{E}_\tau \boldsymbol{\gamma} + \lambda \mathbf{E}_0 \boldsymbol{\gamma} = 0. \tag{3}$$

This is a generalized eigenproblem for which a given eigenvalue λ is interpreted as the ratio of energy at time τ to the initial energy, and the eigenvector $\boldsymbol{\gamma}$ is interpreted as the spectral projection defining the corresponding perturbation.

Our first model assumes that the turbulent channel flow can be adequately represented as a laminar flow with mean velocity profile obeying the law of the wall. The profile used for this investigation is the Reynolds–Tiederman profile chosen by Waleffe and Kim,⁶ defined by

$$\frac{dU}{dy} = -\frac{Ry}{1+G(y)},$$

$$G(y) = \frac{1}{2} \left(1 + \left[\frac{KR}{3} (1-y^2)(1+2y^2) \right]^{1/2} \right) \times \left[1 - \exp\left(-\frac{(1+y)R}{A}\right) \right]^2 - \frac{1}{2}, \quad (4)$$

where $K=0.525$, $A=37$, and with a Reynolds number of $R=180$ based on friction velocity and channel half-width. The profile is symmetrized about $y=0$. For this mean flow, there are no unstable eigenmodes of the linearized Navier-Stokes equations.

The first optimal perturbation we will consider is the global optimal for the flow: the initial disturbance that gains the maximum possible energy from the mean flow before its eventual decay. A search in (α, β, τ) space for the maximum energy growth identifies the global optimal as a streamwise vortex with $\alpha=0$ and $\beta=2.1$ ($\lambda_z^+ = 540$, compared to the observed $\lambda_z^+ \approx 100$), with energy increasing by a factor of 235 at $\tau^+ = 2340$. This disturbance is similar to the Poiseuille flow global optimal,⁹ which occupies the entire width of the flow forming antisymmetric streaks of streamwise velocity roughly centered in the half-channel.

However, the mean flow does not adequately describe the environment felt by a large-scale disturbance developing in turbulent flow. A linear perturbation may develop undisturbed for an unlimited time period in laminar flow, but in turbulent flow the development is disrupted by small-scale turbulent motions on a time scale much shorter than the viscous time scale. The time scale that characterizes this disruption is the eddy turnover time, $\tau_e = q^2/\epsilon$: the ratio of the square of the characteristic turbulent velocity,

$q^2 = \overline{u_i u_i}$ to the dissipation rate, $\epsilon = \overline{v u_i \mu_{i,j} \mu_{i,j}}$.¹⁰ Consequently, we restrict the optimal disturbance development to a time interval consistent with the eddy turnover time near the wall.

In Fig. 1, τ_e is plotted as a function of distance from the wall. Clearly, this plot shows that τ_e near the wall is much shorter than the growth time $\tau^+ = 2340$ of the global optimal. Consequently, we determine the disturbance of maximum energy growth over a time period $\tau^+ = 80$, representative of the eddy turnover time near the wall. The optimal perturbation over this time period is a streamwise vortex ($\alpha=0$) producing the streaks of Fig. 2, with spanwise wavelength $\lambda_z^+ = 110$ nearly equal to the observed spacing and with peak streak velocity at $y^+ \approx 19$.

We now determine the selection rule for this perturbation. The optimal perturbation energy growth as a function of spanwise wavelength for optimization times $\tau^+ = 40, 80$, and 120 is plotted in Fig. 3. The energy growth of the maximally growing perturbation increases with the optimization time, as does its spanwise wavelength. The contours of u are similar to those shown in Fig. 2, with maximum streak velocities for $t^+ = \tau^+ = 40$ and 120 located at $y_c^+ = 14$ and 23, respectively.

The optimization time can be determined by comparing τ as a function of peak streak velocity location y_c^+ to eddy turnover time as a function of y^+ , as shown in Fig. 1. Consider the optimal perturbation for $\tau^+ = 200$. Figure 1 shows that the location of peak streak velocity for this optimal is $y_c^+ = 29$. But the eddy turnover time at $y^+ = 29$ is

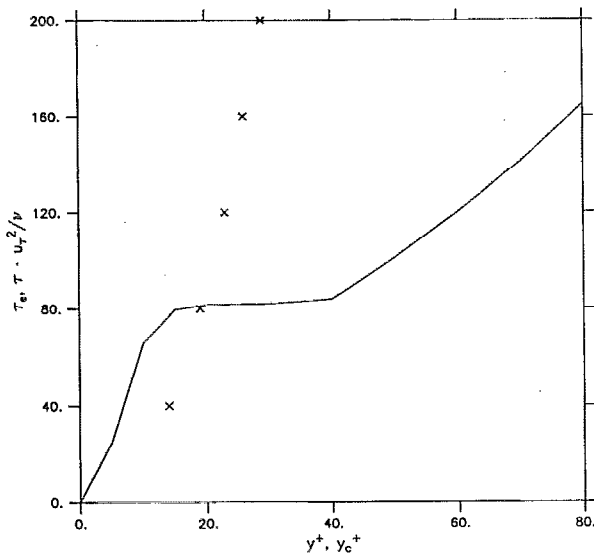


FIG. 1. Eddy turnover time versus distance from wall (—) for turbulent channel flow, estimated from a plot of the shear rate parameter $S^* = S q^2/\epsilon$, where $1/S$ is the time scale of mean deformation.⁵ Also plotted (x) is optimal growth time $t^+ \tau$ versus location of maximum streamwise velocity, y_c^+ at $t^+ = \tau$, for the optimal perturbation over time τ .

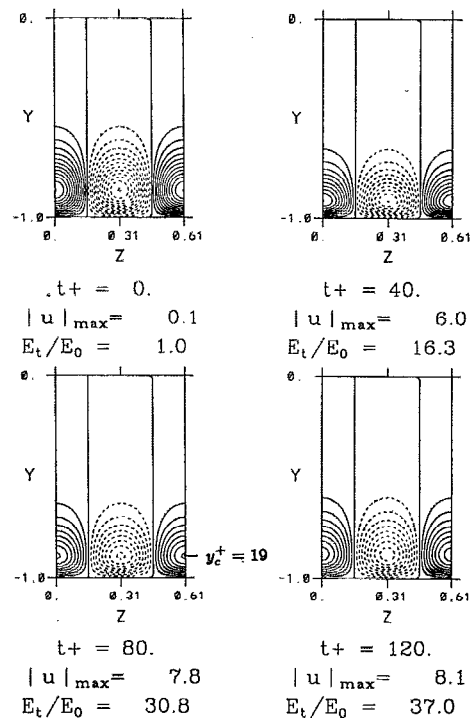


FIG. 2. Development in time of the streamwise velocity u for the perturbation that gains the most energy over the time interval $\tau^+ = 80$. Streamwise and spanwise wave numbers are $\alpha=0$ and $\beta=10.3$, respectively, for a spanwise wavelength of $\lambda_z^+ = 110$.

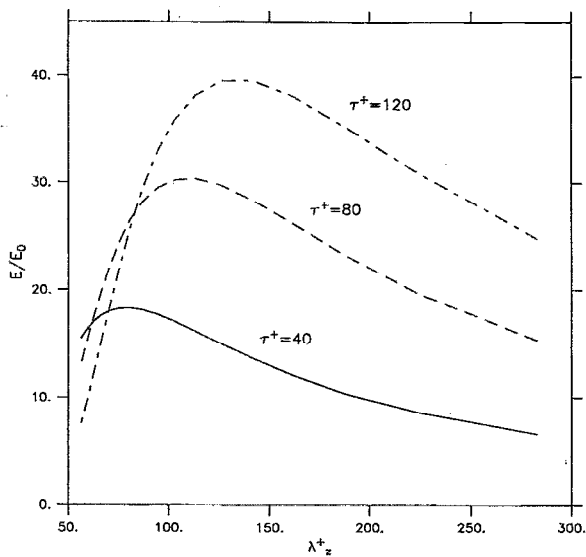


FIG. 3. Optimal energy growth versus wavelength for optimization times representative of the eddy turnover time near the wall.

$\tau_e^+ \approx 80$. So turbulent disruption will not allow the perturbation to reach its full growth. On the other hand, the optimal for $\tau^+ = 40$ has peak streak velocity at $y_c^+ = 14$, where the eddy turnover time is $\tau_e^+ \approx 75$. This perturbation is not highly disrupted over its growth time, although its growth is not as great as that of optimal perturbations with larger τ . The best choice of τ occurs near the intersection of these curves for $\tau^+ \approx 80$. This choice produces the observed spanwise spacing $\lambda_z^+ \approx 100$.

Concentration of energetic perturbations in the near-wall region of high shear is consistent with the previous finding for Blasius flow⁹ in which the optimal perturbations were also found to be streamwise rolls with diameters on the order of the shear-layer thickness.

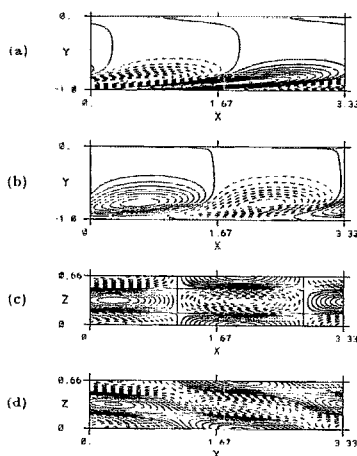


FIG. 4. Optimal perturbation with $(\alpha, \beta, \tau^+) = (1.885, \pm 9.5, 80)$ at time $t^+ = 80$. (a) u in x - y plane, (b) v in x - y plane, (c) u in x - z plane at $y^+ = 15$ for symmetrized optimal obtained from a linear combination of (α, β, τ) and $(\alpha, -\beta, \tau)$ optimals with equal amplitudes, and (d) u in x - z plane at $y^+ = 15$ for asymmetric optimal, with the (α, β, τ) optimal combined with the $(\alpha, -\beta, \tau)$ optimal at one-half amplitude.

Both the location of peak streamwise velocity y_c^+ and the maximum spanwise wave number λ_z^+ increase with τ . This is consistent with the experimental evidence that streak spacing increases with distance from the wall. A further calculation of optimal spanwise wave numbers for the Reynolds-Tiederman profile with $R = 360$ confirmed the insensitivity of the optimal perturbation to changes in Reynolds number.

Streamwise vortices in turbulent flows are observed to extend over streamwise distances of a few hundred wall units. The optimal perturbation with $\tau^+ = 80$ and $\lambda_x^+ = 600$, for which $\lambda_z^+ = 120$, reproduces the shear-layer structures described in Johansson *et al.* (their Fig. 5).¹¹ This perturbation, shown in Fig. 4 at $t^+ = 80$, grows by about 80% of the energy gained by the unconstrained (in x) optimal with $\tau^+ = 80$. The contours of u in the x - y plane, initially of small amplitude, rapidly develop a shear-layer structure consistent with the observations. Peak amplitude is above 80% of that at $t^+ = 80$ over the time period $t^+ = 40$ – 120 , which can be compared to an observed mean survival time for such shear-layer structures of about $t^+ = 50$. The structure propagates at a velocity of $11u_\tau$ measured at $y^+ = 15$, compared to the observed mean velocity of $10.6u_\tau$. As shown in Figs. 4(c) and 4(d), contours of u in the x - z plane similar to symmetric and asymmetric conditional averages in Johansson *et al.* (their Figs. 6 and 13) arise from linear combinations of the energetically equivalent (α, β, τ) and $(\alpha, -\beta, \tau)$ optimals.

Finally, we note that spatial constraints could also be accommodated by the variational method for finding optimals, and that the resulting optimals may also be relevant to understanding coherent structures in boundary layer flows.

In conclusion, we have shown that the $\lambda_z^+ \approx 100$ turbulent streak spacing observed in wall-bounded shear flow is consistent with optimal perturbations constrained to grow maximally over an eddy turnover time.

ACKNOWLEDGMENTS

This work was supported by NSF ATM-8912432, with computer time provided by NCAR 35121031. The National Center for Atmospheric Research is supported by the National Science Foundation.

¹S. J. Kline, W. C. Reynolds, F. A. Schraub, and P. W. Runstadler, "The structure of turbulent boundary layers," *J. Fluid Mech.* **30**, 741 (1967).

²H. T. Kim, S. J. Kline, and W. C. Reynolds, "The production of turbulence near a smooth wall in a turbulent boundary layer," *J. Fluid Mech.* **50**, 133 (1971).

³C. R. Smith and S. P. Metzler, "The characteristics of low-speed streaks in the near-wall region of a turbulent boundary layer," *J. Fluid Mech.* **129**, 27 (1983).

⁴J. Kim, P. Moin, and R. Moser, "Turbulence statistics in fully developed channel flow at low Reynolds number," *J. Fluid Mech.* **177**, 133 (1987).

- ⁵M. J. Lee, J. Kim, and P. Moin, "Structure of turbulence at high shear rate," *J. Fluid Mech.* **216**, 561 (1990).
- ⁶F. Waleffe and J. Kim, "On the origin of streaks in turbulent shear flows," 8th Symposium on Turbulent Shear Flows, 5-5 (1991).
- ⁷L. H. Gustavsson, "Energy growth of three-dimensional disturbances in plane Poiseuille flow," *J. Fluid Mech.* **224**, 241 (1991).
- ⁸D. J. Benney and L. H. Gustavsson, "A new mechanism for linear and nonlinear hydrodynamic instability," *Stud. Appl. Math.* **64**, 185 (1981).
- ⁹K. M. Butler and B. F. Farrell, "Three-dimensional optimal perturbations in viscous shear flow," *Phys. Fluids A* **4**, 1637 (1992).
- ¹⁰H. Tennekes and J. L. Lumley, *A First Course in Turbulence* (MIT Press, Cambridge, MA, 1972).
- ¹¹A. V. Johansson, P. H. Alfredsson, and J. Kim, "Evolution and dynamics of shear-layer structures in near-wall turbulence," *J. Fluid Mech.* **224**, 579 (1991).